ACS Catalysis

Letter

pubs.acs.org/acscatalysis

Water Splitting over Graphene-Based Catalysts: Ab Initio Calculations

D. W. Boukhvalov,*[,†] Y.-W. Son,[†] and R. S. Ruoff[‡,⊥]

[†]School of Computational Sciences, Korea Institute for Advanced Study, Seoul 130-722, Korea

[‡]Department of Mechanical Engineering and the Materials Science and Engineering Program, The University of Texas, Austin, Texas 78712, United States

ABSTRACT: We present first-principles modeling of water oxidation over various graphene systems, such as nitrogen-doped graphene; graphene monolayers on iron, nickel, and copper surfaces; and bi- and trilayer graphene on copper surfaces. It is shown that nitrogen-doped graphene and graphene over copper are better for this reaction than those over platinum at temperatures below 100 °C. Bi- and trilayer graphene on copper have catalytic properties similar to those of a monolayer on copper.

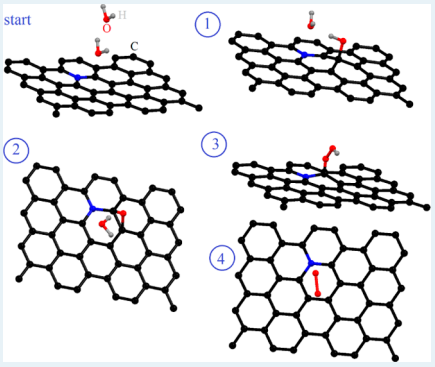

KEYWORDS: *graphene, water splitting, oxidation, carbocatalysis, DFT, modeling*

Water splitting has been proposed as the best route to produce hydrogen for use in energy and chemistry.[1−3] The two main routes are photocatalytic "water splitting" (also known as artificial photosynthesis)[4,5] and electrochemical water splitting. Both critically depend on catalysis if they are to be useful. Electrochemical water splitting is expected to be a key method for producing hydrogen as a fuel for transportation vehicles, and there are several requirements for the electrodes to achieve this goal: (i) they should have high efficiency, (ii) they should be made from low cost and abundant materials,[1−3] and (iii) they should be stable over many cycles of the reaction.[6] Recent experimental and theoretical studies have proposed either platinum or iridium oxides as the most efficient catalysts for electrochemical water splitting,[7−10] but low abundance, high cost, and surface poisoning[11−13] suggest that these catalysts cannot be used on a large scale. This motivates study on other potential catalysts for water splitting.

Recent experimental[14−36] and theoretical[37−39] studies have demonstrated the catalytic activity of chemically modified graphene for various reactions, such as the oxidation and hydration of many organic molecules, hydrogenation of magnesium, and for the oxygen reduction reaction. A doped metal substrate with a graphene overlayer[37] or graphene substitutionally doped with nitrogen atoms (N-doped graphene)[39] can lower energy barriers for certain reactions. As a specific example, the dissociation of molecular hydrogen on graphene-like layers on the surfaces of nickel nanoparticles has been studied both experimentally and theoretically.[37] Recent progress in large-scale production of N-doped graphene[14−24] and graphene on metal substrates[40−43] may enable these materials to eventually play a role as industrial catalysts. In view of this rapid development in the field, a detailed understanding of catalytic reactions for water splitting in various modified graphene systems is called for. In this work, we perform ab initio calculations to study water splitting using N-doped graphene or graphene-coated metals.

The water-splitting reaction is usually described as a four-step process,[44,45] and we have modeled the reaction in the modified graphene systems in the conventional way. These steps, shown in Figure 1, can be briefly described as (1) a water molecule reacting with graphene to produce hydroxide-functionalized graphene and a proton in water; (2) the hydroxide-functionalized graphene loses a second hydrogen proton, producing epoxide-functionalized graphene; (3) a second water molecule reacts with the epoxide to produce a third free hydrogen proton and peroxide-functionalized graphene; and finally, (4) the peroxide separates from the graphene layer, forming a free oxygen molecule and a fourth free hydrogen proton. For N-doped graphene, the nitrogen concentration in our model was fixed at 2 at. % (see Figure 1) as was done in our previous theoretical study[39] and in other experimental work.[25] For graphene on a metal substrate, Fe, Ni, and Cu were studied as model metallic substrates. The substrates were modeled with four layers (24 metal atoms in each layer), and the (111) plane of the face-centered cubic lattice was used as the surface.

Different levels and types of water coverage were studied, as shown in Figure 2. The lowest coverage (Figure 2a) corresponds to water in the gaseous phase. The recently

Received: February 20, 2014
Revised: May 9, 2014
Published: May 12, 2014

   dx.doi.org/10.1021/cs5002288 | ACS Catal. 2014, 4, 2016−2021

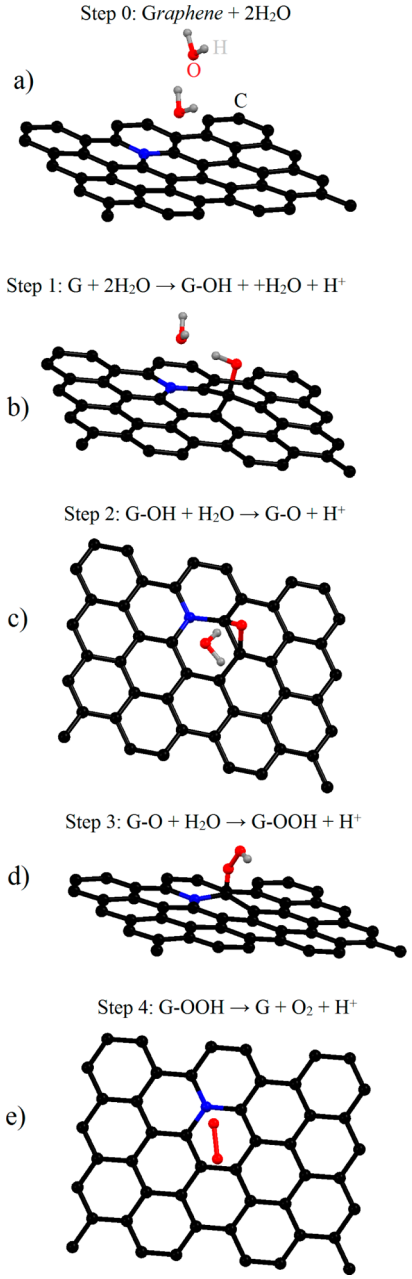

Figure 1. Steps of water splitting over nitrogen-doped graphene for the minimum concentration of water. Protons are omitted so that the figures are clearer.

discussed[46−49] formation of a single layer of "hexagonal ice" on graphene was also taken into account (Figure 2c). A quasirandom distribution of water molecules over the substrate (Figure 2b,d) was used in one set of calculations. We note that our model does not take into account long-range intermolecular interactions that would be present in an exact model of liquid water. We suggest, however, that such interactions may play no significant role in the catalytic reaction process because the binding energy of water−water interactions in liquid water (about 0.1 eV per H bond) is much smaller than the difference between energies for each of the four steps of the water-splitting reaction (see Figure 2). For liquid water, we examined two possibilities: water molecules that cover (i) a half or (ii) all of the catalyst surface (Figure 2b,d).

We used density functional theory (DFT) as implemented in the pseudopotential code SIESTA,[50] as in our previous studies.[37−39] All calculations were performed using the generalized gradient approximation (GGA-PBE) with spin-polarization[51] and implementation of the correction of van der Waals forces.[52] During the optimization, the ion cores were described by norm-conserving nonrelativistic pseudopotentials[53] with cut off radii 1.14, 1.45, 1.25, and 2.15 au for C, N, H, and transition metals, respectively, and the wave functions were expanded with localized orbitals and double-ζ basis set for hydrogen and a double-ζ plus polarization basis set for other species. Full optimization of the atomic positions was performed. Optimization of the force and total energy was performed with an accuracy of 0.04 eV/Å and 1 meV, respectively. All calculations were carried out with an energy mesh cutoff of 360 Ry and a k-point mesh of 8 × 6 × 2 in the Monkhorst−Pack scheme.[54] We found that the optimized distance between the metal surface and graphene obtained in our calculations shows good agreement with experimental results.[43]

For electrochemical reactions, the free energy diagram provides a basis for discussion of the reactions. The free energies were calculated in the same manner as previously used for platinum-based water splitting[4] with the formula: $G = \Delta E_N - neU + E_{ZP}$, where ΔE_N is the energy difference (per water molecule involved in the current step or reaction) between the total energies at the N and N − 1 steps of the reaction being modeled, e is the electron charge, U is an equilibrium potential, n is the number of hydrogen atoms, and E_{ZP} is the zero-point energy correction. The values of U (1.23 eV) and zero-point energy corrections are the same as those previously used.[7−9,44,45] The "perfect" catalyst would yield free energies equal to zero at each reaction step according to the equation:

$$2H_2O + 4 \times 1.23\ \text{eV} \rightarrow O_2 + 4H^+ + 4e^-$$

as discussed in detail in ref 9. A "good" catalyst will be one in which the free energies of each step are close to zero. The free energy differences for each reaction step are "energy costs" for that reaction step. Note that by using the value of U = 1.23 eV, the fourth step always corresponds to zero free energy, and we omit it for clarity in Figures 2 and 3. The relation between the calculated energy costs and reaction temperatures using graphene catalysts are discussed below. Because our previous calculations suggest a dramatic decrease of the activation energy (the energy required for the transformation of an O═O molecule to −O-O- prior to the formation of two epoxy groups on graphene) over doped graphene[39] and an insignificant increase (∼0.2 eV) of the total energy of similar systems at intermediate states of reactions catalyzed by graphene oxide,[38] we will not further discuss the energetics of the other intermediate steps in this work. We also checked the role of H^+ by performing calculations of the energy barriers for the reaction shown in Figure 1 using the ASE code[55] and obtained values of energy barriers below 0.18 eV.

The results (Figure 2) show that on the N-doped graphene or the graphene-on-metal, in contrast to the Pt surface, the first and the last steps of the overall water-splitting reaction (i.e., the formation of a hydroxyl group, Figure 1b, and −OOH groups, Figure 1d) are more energetically favorable than the second step (formation of epoxy groups, Figure 1c) for all water configurations studied. This is a fundamental difference between metal-based catalysts (pure metals, metal oxides, and similar compounds, and metal atoms inserted in a nonmetallic

dx.doi.org/10.1021/cs5002288 | ACS Catal. 2014, 4, 2016−2021

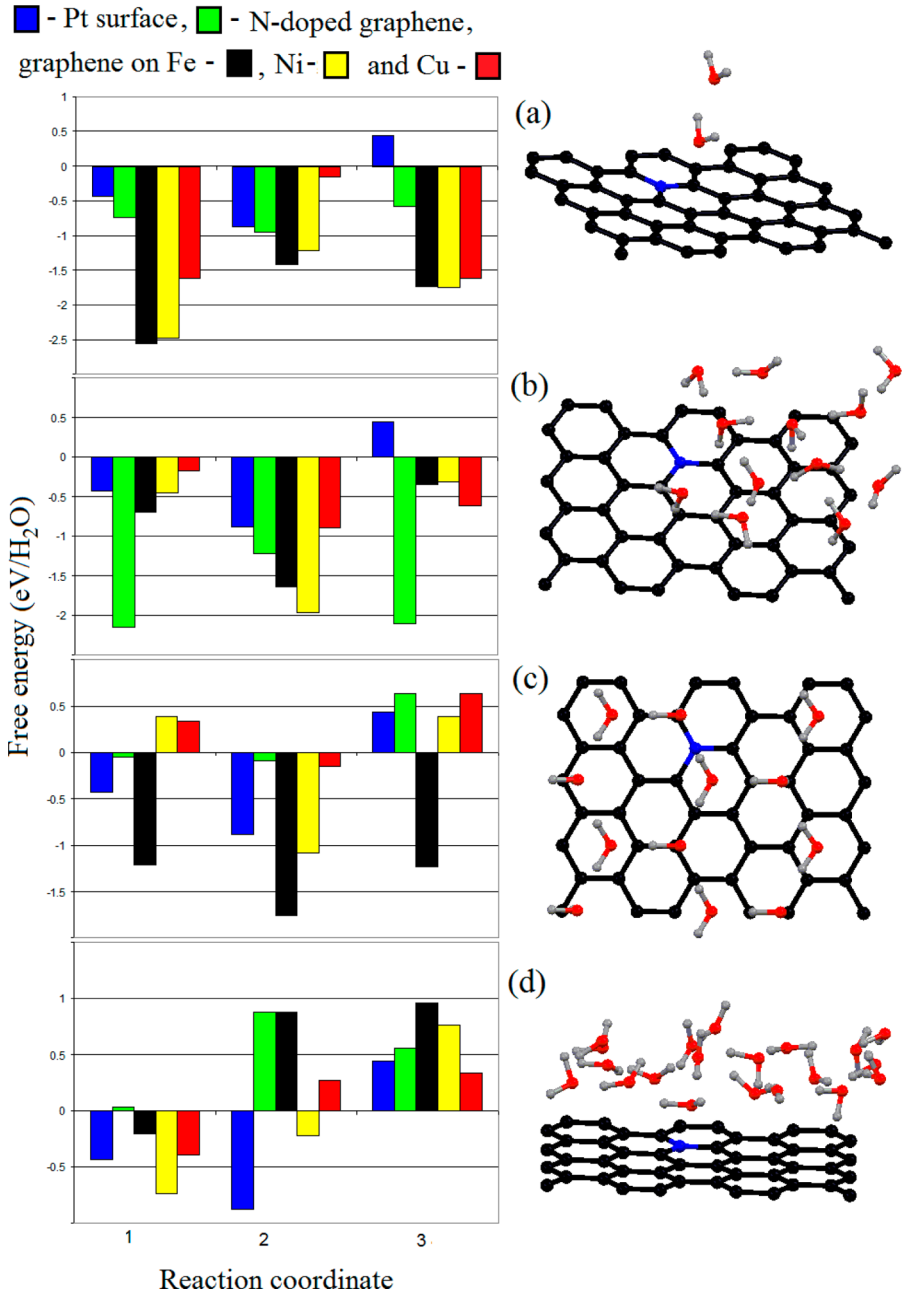

Figure 2. Free energy diagrams for the reaction steps shown in Figure 1 for U = 1.23 eV as a function of catalyst material and the water configuration. The values of free energies of the reaction over a Pt surface are taken from ref 18. Note that by using the value of U = 1.23 eV, the fourth step always corresponds to zero free energy, and we later omit it for clarity.

matrix)[56] and catalysts based on graphene. In the case of pure metals, the adsorption of molecular species cannot break any bonds in the metal or reduce a metal oxide (in which a change of the oxidation states of multivalent metal atoms takes place). On the other hand, in graphene, the adsorption of a single monovalent species, such as hydrogen, fluorine, or a hydroxyl group, requires a double bond to break, with the consequent appearance of an unpaired electron in the graphene.[57] The nitrogen atom in N-doped graphene provides a hole, and the underlying metal substrate for the graphene-on-metal catalyst can inject an electron into the graphene layer. These additional charge carriers compensate for the unpaired electron that appears after adsorption of a single monovalent group. Note that for pristine graphene (defined here as undoped and free-standing graphene), the first step of the overall water-splitting reaction is very unfavorable. We found that the configuration shown in Figure 1d is extremely unstable for pristine graphene and, indeed, cannot be obtained using the DFT calculations. Independent of the starting atomic position, the −OOH group detaches from graphene and moves to a distance more that 3 Å away from the substrate.

Unlike the catalytic reaction on platinum, increasing the concentration of water molecules at the surface favors water-splitting on graphene-based catalysts. Some recent theoretical work discusses the charge transfer from water molecules to hydroxyl groups on graphene, and this effective doping from water molecules provides partial compensation for the dangling bonds and increases the mobility of hydroxyl groups on

dx.doi.org/10.1021/cs5002288 | ACS Catal. 2014, 4, 2016−2021

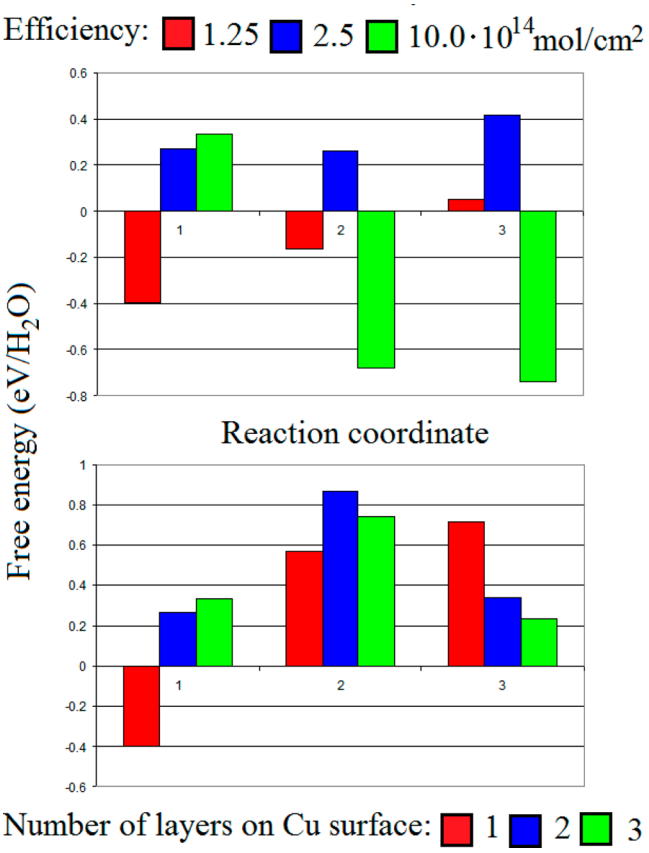

Figure 3. Free energy diagrams for the reaction steps shown in Figure 1 for U = 1.23 eV using a graphene-on-copper catalyst as a function of (a) efficiency and (b) number of graphene layers.

graphene.[58] In the case of water-splitting reactions, this additional doping can also facilitate the first and third steps of the reactions discussed above for doping from metal substrates. We can also see that as the period of the elements used as the substrate increases from iron to copper, the energy costs of the water-splitting steps decreases. This effect is caused by the increased occupancy of the metal 3d shell that increases the effective electron doping in the graphene layer. Another source of this effect is the weakening of the graphene/substrate bonding[37] from iron to copper that increases the mechanical flexibility of the graphene membrane, which plays an important role in its chemical activity.[57] Here, we note one crucial difference between graphene and metal-based catalysts, namely, that in the case of the direct use of metals and alloys as catalysts, the exact composition of the metal plays the key role.[44,45] However, in graphene-covered metal substrates, metal−graphene binding and the total level of doping of the graphene are pivotal, that is, the exact composition of the substrate alloy and the quality of the metallic surface are not so important.

To estimate the possibility of using graphene-based catalysts for practical water splitting, the temperature of the process needs to be considered. The process of electrochemical water splitting provides unavoidable heating of the electrolytes,[59] and the type of materials used in the catalyst can limit the maximum temperature attained during this process. Currently, polymer electrolyte membrane (PEM)-based devices, which have been proposed as the most promising for large-scale realization of this process,[60] exhibit reactions that occur at temperatures between 20 and 200 °C,[61] corresponding to calculated energy costs of the reactions below 0.5 and 1.2 eV, respectively. These values were deduced earlier on the basis of our work that compared the experimental reaction temperatures and calculated energies of various chemical reactions on a graphene oxide substrate.[38] From the results of calculations, for the case of low concentrations of water, only Pt and N-doped graphene are feasible catalysts. For increased water concentrations, however, graphene-on-Ni and especially graphene-on-Cu become rather attractive for water splitting. In the case of the maximum water concentration (Figure 2d) graphene-on-copper is a better catalyst than platinum and is suitable for low-temperature water splitting (the energy required for each step of the multistep reaction is below 0.5 eV). For this catalyst, we thus checked the maximum efficiency. We have calculated the splitting of four and eight water molecules over the same supercell of graphene (48 carbon atoms, see Figure 1) and find that increasing the number of active centers requires higher energies (∼0.75 eV/H_2O; see Figure 3a). Thus, increasing the water-splitting temperature from 50 to 100 °C will increase the hydrogen output from a graphene-on-copper catalyst by a factor of 4.

The last step of our survey is motivated by the recent experimental results of the increased oxidation of copper foils over a long time period, after coverage by a graphene monolayer grown by CVD[62,63] that encouraged us also to model an increased number of graphene layers. Another reason for the exploration of the few-layer case is the possible use of graphene-based catalysts with multilayer graphene by industry. Increasing the number of layers decreases the chemical activity of graphene,[37,57] and the surface of graphite is much less chemically active than that of graphene. Thus, increasing the number of graphene layers could break the process of copper oxidation. We have checked the influence of increasing the number of graphene layers in regard to the energetics of electrochemical water splitting (Figure 3b) and found that the second and third graphene layers on a copper substrate provide an insignificant change in the energy costs of these reactions, and the computed energies suggest that using a few layers of graphene on copper as a catalyst for hydrogen production is still viable at low temperatures (below 100 °C).

The results of this first-principles modeling demonstrate the good capability of these graphene-based materials as catalysts of water splitting. There are two possible candidates for replacing the current rare and high cost catalysts: namely, nitrogen-doped graphene and graphene over a copper substrate. The latter can be used for hydrolysis at temperatures below 100 °C and should have no limitations caused by corrugation in the graphene layer, unlike nitrogen-doped graphene.[39] Increasing the process temperature to 100 °C results in reactions over larger areas of graphene and an increased overall rate of reaction and also permits the use of a few layers of graphene (as opposed to a monolayer), which should be more chemically stable.

AUTHOR INFORMATION

Corresponding Author

*E-mail: danil@kias.re.kr.

Present Address

[⊥](R.S.R.) Center for Multidimensional Carbon Materials, Institute for Basic Science (IBS), and Department of Chemistry, Ulsan National Institute of Science and Technology (UNIST), Ulsan 689-798, Republic of Korea.

dx.doi.org/10.1021/cs5002288 | *ACS Catal.* 2014, 4, 2016−2021

Notes

The authors declare no competing financial interest.

■ ACKNOWLEDGMENTS

Y.-W.S. was supported by the NRF of Korea Grant funded by the MSIP (CASE, 2011-0031640). R.S.R. acknowledges financial support by the Research Center Program of the Institute for Basic Science (IBS) in Korea. Computations were supported by the CAC of KIAS.

■ REFERENCES

(1) Bockris, J. O.; Veziroglu, T. N. *Int. J. Hydrogen Energy* **2007**, *32*, 1605−1610.
(2) Suh, M. P.; Park, H. J.; Prasad, T. K.; Lim, D.-W. *Chem. Rev.* **2012**, *112*, 782−835.
(3) Eberle, U.; Felderhoff, M.; Schüth, F. *Angew. Chem., Int. Ed.* **2009**, *48*, 6608−6630.
(4) Gust, D.; Moore, T. A.; Moore, A. L. *Acc. Chem. Res.* **2009**, *42*, 1890−1898.
(5) Kudo, A.; Miseki, Y. *Chem. Soc. Rev.* **2009**, *38*, 253−278.
(6) Nikiforov, A. V.; Petrushina, I. M.; Christensen, E.; Tomás-García, A. L.; Bjerrum, N. J. *Int. J. Hydrogen Energy* **2011**, *36*, 111−119.
(7) Stamenkovic, V.; Mun, B. S.; Mayrhofer, K. J. J.; Ross, P. N.; Markovic, N. M.; Rossmeisl, J.; Greeley, J.; Nørskov, J. K. *Angew. Chem., Int. Ed.* **2006**, *45*, 2897−2901.
(8) Rossmeisl, J.; Logadottir, A.; Nørskov, J. K. *Chem. Phys.* **2005**, *319*, 178−184.
(9) Man, I. C.; Su, H.-Y.; Calle-Vallejo, F.; Hansen, H. A.; Martinez, J. I.; Inoglu, N. G.; Kitchin, J.; Jaramillo, T. F.; Nørskov, J. K.; Rossmeisl, J. *ChemCatChem* **2011**, *3*, 1159−1165.
(10) Tilley, S. D.; Cornuz, M.; Sivula, K.; Grätzel, M. *Angew. Chem.* **2010**, *122*, 6549−6552.
(11) Li, Q.; He, R.; Gao, J.-A.; Jensen, J. O.; Bjerrum, N. J. *J. Electrochem. Soc.* **2003**, *150*, A1599−A1605.
(12) Grunes, J.; Zhu, J.; Yang, M.; Somorjai, G. A. *Catal. Lett.* **2003**, *86*, 157−161.
(13) Su, D. S.; Perathoner, S.; Centi, G. *Chem. Rev.* **2013**, *113*, 5782−5816.
(14) Matter, P. H.; Zhang, L.; Ozkan, U. S. *J. Catal.* **2006**, *239*, 83−96.
(15) Matter, P. H.; Wang, E.; Arias, M.; Biddinger, E. J.; Ozkan, U. S. *J. Mol. Catal. A: Chem.* **2007**, *264*, 73−81.
(16) Niwa, H.; Horiba, K.; Harada, Y.; Oshima, M.; Ikeda, T.; Terakura, K.; Ozaki, J.; Miyata, S. *J. Power Sources* **2009**, *187*, 93−97.
(17) Xiong, W.; Du, F.; Liu, Y.; Perez, A., Jr.; Supp, M.; Ramakrishnan, T. S.; Dai, L.; Jiang, L. *J. Am. Chem. Soc.* **2010**, *132*, 15839−15841.
(18) Tang, Y.; Allen, B. L.; Kauffman, D. R.; Star, A. *J. Am. Chem. Soc.* **2009**, *131*, 13200−13201.
(19) Maldonado, S.; Stevenson, K. J. *J. Phys. Chem. C* **2005**, *109*, 4707−4716.
(20) Kundu, S.; Chikka, T.; Xia, W.; Wang, Y.; Van Dommele, S.; Hendrik, J.; Santa, M.; Grundmeier, G.; Bron, M.; Schuhmann, W.; Muhler, M. *J. Phys. Chem. C* **2009**, *113*, 14302−14310.
(21) Chen, Z.; Higgins, D.; Tao, H.; Hsu, R. S.; Chen, Z. *J. Phys. Chem. C* **2009**, *113*, 21008−21013.
(22) Nagaiah, T. C.; Kundu, S.; Bron, M.; Muhlen, M.; Schuhmann, W. *Electrochem. Commun.* **2010**, *12*, 338−341.
(23) Subramanian, N. P.; Li, X.; Nallathambi, V.; Kumaraguru, P.; Colon-Mercado, H.; Wu, G.; Lee, J.-W.; Popov, B. N. *J. Power Sources* **2009**, *188*, 38−44.
(24) Qu, L.; Liu, Y.; Baek, J.-B.; Dai, L. *ACS Nano* **2010**, *4*, 1321−1326.
(25) Yang, S.; Feng, X.; Wang, X.; Müllen, K. *Angew. Chem., Int. Ed.* **2011**, *50*, 5339−5343.
(26) Panchakarla, L. S.; Subrahmanyam, K. S.; Saha, S. K.; Govindaraj, A.; Krishnamurthy, H. R.; Waghmare, U. V.; Rao, C. N. R. *Adv. Mater.* **2009**, *21*, 4726−4730.
(27) Sheng, Z.-H.; Gao, H.-L.; Bao, W.-J.; Wang, F.-B.; Xia, X.-H. *J. Mater. Chem.* **2012**, *22*, 390−395.
(28) Lin, T.; Huang, F.; Liang, J.; Wang, Y. *Energy Environ. Sci.* **2011**, *4*, 862−865.
(29) Yang, Z.; Yao, Z.; Li, G.; Fang, G.; Nie, H.; Liu, Z.; Zhou, X.; Chen, X.; Huang, S. *ACS Nano* **2012**, *6*, 205−211.
(30) Yang, S.; Zhi, L.; Tang, K.; Feng, X.; Maier, J.; Müllen, K. *Adv. Funct. Mater.* **2012**, *22*, 3634−3640.
(31) Liang, J.; Jiao, Y.; Jaroniec, M.; Qiao, S. Z. *Angew. Chem., Int. Ed.* **2012**, *51*, 11496−11500.
(32) Dreyer, D. R.; Jia, H.-P.; Bielawski, C. W. *Angew. Chem., Int. Ed.* **2010**, *49*, 6813−6818.
(33) Jia, H.-P.; Dreyer, D. R.; Bielawski, C. W. *Tetrahedron* **2011**, *67*, 4431−4434.
(34) Jia, H.-P.; Dreyer, D. R.; Bielawski, C. W. *Adv. Synth. Catal.* **2011**, *353*, 528−532.
(35) Dreyer, D. D.; Jia, H.-P.; Todd, A. D.; Geng, J.; Bielawski, C. W. *Org. Biomol. Chem.* **2011**, *9*, 7292−7295.
(36) Su, C. L.; Acik, M.; Takai, K.; Lu, J.; Hao, S.-J.; Zheng, Y.; Wu, P. P.; Bao, Q. L.; Enoki, T.; Chabal, Y. J.; Loh, K. P. *Nat. Commun.* **2012**, *3*, 1298.
(37) Yermakov, A. Ye.; Boukhvalov, D. W.; Uimin, M. A.; Lokteva, E. S.; Erokhin, A. V.; Schegoleva, N. N. *ChemPhysChem* **2013**, *14*, 381−385.
(38) Boukhvalov, D. W.; Dreyer, D. R.; Bielawski, C. W.; Son, Y.-W. *ChemCatChem* **2012**, *4*, 1844.
(39) Boukhvalov, D. W.; Son, Y.-W. *Nanoscale* **2012**, *4*, 417−420.
(40) Wei, D.; Wu, B.; Guo, Y.; Liu, Y. *Acc. Chem. Res.* **2013**, *46*, 106−115.
(41) Zhang, Y.; Zhang, L.; Zhou, C. *Acc. Chem. Res.* **2013**, *46*, 2329−2339.
(42) Yan, K.; Fu, L.; Peng, H.; Liu, Z. *Acc. Chem. Res.* **2013**, *46*, 2263−2274.
(43) Seah, C.-M.; Chai, S.-P.; Mohamed, A. R. *Carbon* **2014**, *70*, 1−12.
(44) Hansen, H. A.; Rossmeisl, J.; Nørskov, J. *Phys. Chem. Chem. Phys.* **2008**, *10*, 3722−3730.
(45) Nørskov, J.; Rossmeisl, J.; Logadottir, A.; Lindqvist, L.; Kitchin, J. R.; Bligaard, T.; Jónsson, H. *J. Phys. Chem. B* **2004**, *108*, 17886−17892.
(46) Kimmel, G. A.; Mattheisen, J.; Baer, M.; Mundy, C. J.; Petrik, N. G.; Smith, R. S.; Dohnálek, Z.; Kay, B. D. *J. Am. Chem. Soc.* **2009**, *131*, 12838−12844.
(47) Kim, J.-S.; Choi, J. S.; Lee, M. J.; Park, B. H.; Bukhvalov, D.; Son, Y.-W.; Yoon, D.; Cheong, H.; Park, J. Y.; Salmeron, M. *Sci. Rep.* **2013**, *3*, 2309.
(48) Boukhvalov, D. W.; Katsnelson, M. I.; Son, Y.-W. *Nano Lett.* **2013**, *13*, 3930−3935.
(49) Zheng, Y.; Su, C.; Lu, J.; Loh, K. P. *Angew. Chem., Int. Ed.* **2013**, *52*, 8708−8712.
(50) Soler, J. M.; Artacho, E.; Gale, J. D.; Garsia, A.; Junquera, J.; Orejon, P.; Sanchez-Portal, D. *J. Phys.: Condens. Matter* **2002**, *14*, 2745−2779.
(51) Perdew, J. P.; Burke, K.; Ernzerhof, M. *Phys. Rev. Lett.* **1996**, *77*, 3865−3868.
(52) Dion, M.; Rydberg, H.; Schröder, H.; Langreth, D. C.; Lundqvist, B. I. *Phys. Rev. Lett.* **2004**, *92*, 246401.
(53) Troullier, O. N.; Martins, J. L. *Phys. Rev. B* **1991**, *43*, 1993−2006.
(54) Monkhorst, H. J.; Park, J. D. *Phys. Rev. B* **1976**, *13*, 5188−5192.
(55) https://wiki.fysik.dtu.dk/ase/.
(56) Kaukonen, M.; Krasheninnikov, A. V.; Kauppinen, E.; Nieminen, R. M. *ACS Catal.* **2013**, *3*, 159−165.
(57) Boukhvalov, D. W. *RSC Adv.* **2013**, *3*, 7150−7159.
(58) Boukhvalov, D. W. *Phys. Chem. Chem. Phys.* **2010**, *12*, 15367−15371.
(59) Nikiforov, A. V.; Petrushina, I. M.; Christensen, E.; Alexeev, N. V.; Samokhin, A. V.; Bjerrum, N. J. *Int. J. Hydrogen Energy* **2012**, *37*, 18591−18597.

(60) Zeng, K.; Zhang, D. *Prog. Energy Combust. Sci.* **2010**, *36*, 307−312.
(61) Polonskỳ, J.; Petrushina, I. M.; Christensen, E.; Bouzek, K.; Prag, C. B.; Andersen, J. E. T.; Bjerrum, N. J. *Int. J. Hydrogen Energy* **2011**, *37*, 2173−2181.
(62) Schriver, M.; Regan, W.; Gannet, W. J.; Zaniewski, A. M.; Crommie, M. F.; Zettl, A. *ACS Nano* **2013**, *7*, 5763−5768.
(63) Zhou, F.; Li, Z.; Shenoy, G. J.; Liu, H. *ACS Nano* **2013**, *7*, 6939−6947.

dx.doi.org/10.1021/cs5002288 | *ACS Catal.* 2014, 4, 2016−2021